

## Lifetime Measurements in the Superdeformed Band of $^{192}\text{Hg}$

E. F. Moore, R. V. F. Janssens, I. Ahmad, M. P. Carpenter, P. B. Fernandez, T. L. Khoo, S. L. Ridley,<sup>(a)</sup>  
and F. L. H. Wolfs

*Argonne National Laboratory, Argonne, Illinois 60439*

D. Ye, K. B. Beard, and U. Garg

*University of Notre Dame, Notre Dame, Indiana 46556*

M. W. Drigert

*Idaho National Engineering Laboratory, EG&G Idaho Inc., Idaho Falls, Idaho 83415*

Ph. Benet and P. J. Daly

*Purdue University, West Lafayette, Indiana 47907*

R. Wyss

*Manne Siegbahn Institute of Physics, S-10405 Stockholm, Sweden  
and Royal Institute of Technology, S-10444 Stockholm, Sweden*

W. Nazarewicz

*Institute of Physics, Warsaw University of Technology, PL 00-662 Warsaw, Poland  
(Received 28 March 1990)*

Lifetimes were measured for transitions in the superdeformed band of  $^{192}\text{Hg}$  with the Doppler-shift attenuation method. The results yield an essentially constant quadrupole moment of  $20 \pm 2 e b$  and indicate that the sidefeeding lifetimes are of the same order as the state lifetimes. The data are consistent with calculations using the cranked Woods-Saxon Strutinsky method with pairing.

PACS numbers: 23.20.Ck, 21.10.Ft, 21.10.Re, 27.80.+w

A wealth of information has recently become available on the properties of superdeformed (SD) nuclei, i.e., nuclei trapped in a secondary minimum of the nuclear potential associated with very elongated ellipsoidal shapes.<sup>1</sup> An interesting question concerns the stability of this secondary minimum under the stress of rapid rotation. Perhaps this question is best addressed in nuclei with  $A \sim 190$ . The dynamic moments of inertia  $\mathcal{J}^{(2)}$  of SD bands in all Hg nuclei with  $189 \leq A \leq 194$  have been found<sup>2-5</sup> to show similar increases with rotational frequency  $\hbar\omega$ , and a change in deformation as a function of rotational frequency (centrifugal stretching) is a possible explanation. However, mean-field calculations which attempt to reproduce the variations of  $\mathcal{J}^{(2)}$  with  $\hbar\omega$  have suggested that two other major factors may contribute separately or cooperatively to the observed increase: (i) changes in pairing at large deformations<sup>6</sup> and (ii) occupation of specific high- $j$  intruder orbitals.<sup>6,7</sup> It is the purpose of this Letter to examine these various possibilities through the measurement of the transition quadrupole moments  $Q_t$  in the SD band of  $^{192}\text{Hg}$ .

Lifetimes within the SD band in  $^{192}\text{Hg}$  were measured with the Doppler-shift attenuation method (DSAM). In contrast with previous measurements, where only fractional Doppler shifts  $F(\tau)$  are reported,<sup>1,2</sup> we have been able to analyze detailed line shapes for individual transitions between SD states ( $\beta_2 \sim 0.5$ ). [Another detailed

line-shape analysis of states with large deformation has been performed in  $^{135}\text{Nd}$  ( $\beta_2 \sim 0.4$ ).<sup>8</sup>] Analysis of individual line shapes allows one to determine the variation of  $Q_t$  as a function of  $\hbar\omega$ , as opposed to previous studies where  $Q_t$  was assumed to be constant for all states in the band. In addition, information is also obtained on the feeding times into the SD structure. In this way, the possible causes for the variation in  $\mathcal{J}^{(2)}$  can be checked. In particular, the deformation is shown to remain constant with  $\hbar\omega$ . Our results are compared with Woods-Saxon calculations where the variations of the deformation parameters ( $\beta_2, \beta_4$ ) and of  $\mathcal{J}^{(2)}$  with  $\hbar\omega$  are investigated.

The experiment was carried out at the Argonne Tandem-Superconducting Linear Accelerator System (ATLAS) with the use of 159-MeV  $^{36}\text{S}$  beams to populate the states of  $^{192}\text{Hg}$  with the  $^{160}\text{Gd}(^{36}\text{S}, 4n)$  reaction. The target was a  $990\text{-}\mu\text{g}/\text{cm}^2$  isotopically enriched foil on which  $14\text{-mg}/\text{cm}^2$  Au had been evaporated in order to slow down and finally stop the recoiling nuclei. The choice of the beam energy was dictated by the need to optimize the population of the SD band<sup>9</sup> while keeping reactions from the Au backing to a minimum. The  $\gamma$  rays were observed with the Argonne-Notre Dame  $\gamma$ -ray facility consisting of twelve Compton-suppressed Ge detectors and a fifty-element bismuth-germanate (BGO) array. With a threshold of four on the number of array

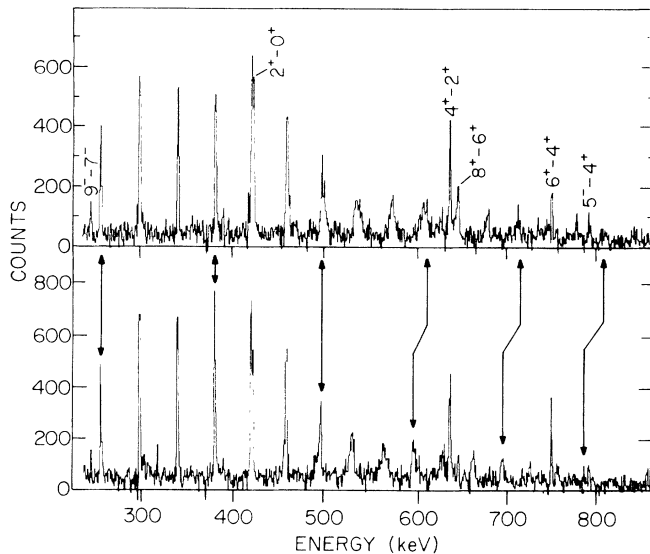


FIG. 1. Coincidence spectra for the SD band in  $^{192}\text{Hg}$  measured at forward (upper part) and backward (lower part) angles. The arrows show the position of the SD transitions and indicate the changes in Doppler shift within the band. Broadened shapes can be seen for  $458 \leq E_\gamma \leq 700$  keV. Transitions with  $E_\gamma \geq 700$  keV show Doppler shifts only, while those with  $E_\gamma \leq 420$  keV exhibit no shifts because they are emitted from stopped  $^{192}\text{Hg}$  nuclei.

elements firing in coincidence with at least two Compton-suppressed Ge detectors, a total of  $9.0 \times 10^7$  events were recorded and stored on magnetic tape for subsequent analysis.

In the analysis,  $\gamma$ - $\gamma$  coincidence matrices were created for all angle combinations (four Ge detectors are located at each of the following three angles:  $34.5^\circ$ ,  $90^\circ$ , and  $145.5^\circ$  with respect to the beam), with an additional condition on the fold data from the inner array in order to enhance the reaction channel of interest (see Ye *et al.*<sup>4</sup> for details). The spectra shown in Fig. 1 were generated by adding spectra obtained in coincidence with the four lowest  $\gamma$  rays in the SD band (257–381 keV) which decay after the residues have stopped in the Au backing. The spectra clearly illustrate that the transitions with energies higher than 420 keV not only exhibit a Doppler shift, when data at forward and backward angles are compared, but that for transitions with  $458 \leq E_\gamma \leq 700$  keV an analysis in terms of broadened line shapes is possible.

In order to extract lifetimes from these broadened line shapes, the computer code LILIFI<sup>10,11</sup> was used. The electronic and the nuclear components of the stopping power were calculated with the code TRIM85<sup>12</sup> which uses the most recent and complete evaluation of existing stopping-power data. The detailed slowing down history in both the target and Au backing includes the effects of lateral and longitudinal straggling;  $10^4$  recoiling  $^{192}\text{Hg}$  ions were traced in a Monte Carlo simulation. Correc-

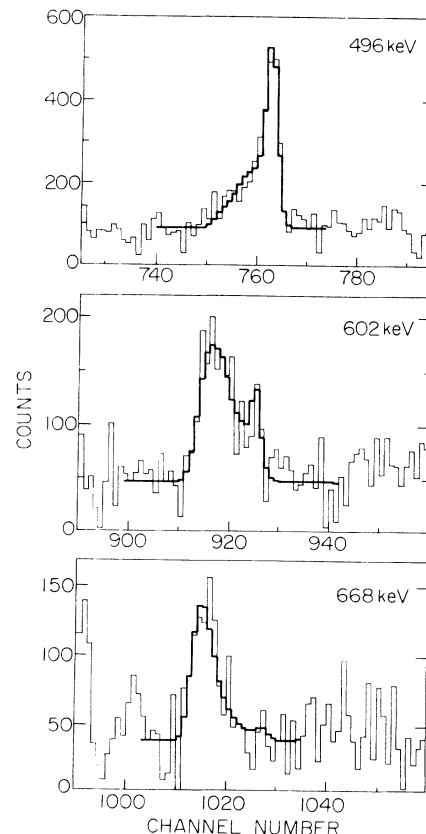


FIG. 2. Examples of fits (thick line) to three transitions in the SD band as measured at backward angles. The data are represented with the thin lines.

tions for the finite solid angle of the Ge detectors and the positional dependence of their efficiencies are also included in the analysis. The calculated line shapes take into account (a) the decay within the SD band (with known transition energies and  $\gamma$ -ray intensities); (b) a set of precursor rotational transitions (with the same moment of inertia) preceding the highest known SD transition; and (c) sidefeeding into each state, approximated by a single rotational cascade of 5–8 transitions. The lifetimes within the feeder bands were controlled by a single parameter  $(Q_i^2/\mathcal{I}^5)_{\text{SF}}$ , where  $(Q_i)_{\text{SF}}$  and  $\mathcal{I}_{\text{SF}}$  are effective quadrupole moments and moments of inertia for the sidefeeding cascades.<sup>13</sup> For each line shape, both the state lifetime and the sidefeeding parameter are derived from the fit. The spectra measured at all three angles were analyzed. Examples of fits obtained at backward angles for selected transitions are presented in Fig. 2. Simultaneous fits to successive transitions were performed in order to determine correlations between fit parameters. Table I summarizes our results. Statistical errors are included in Table I, while systematic errors in the treatment of the slowing-down process, which could be as large as (15–20)%, have been omitted.

As illustrated in Fig. 2, the measured line shapes are

TABLE I. Summary of lifetime,  $B(E2)$ , and transition quadrupole moment information for the SD band in  $^{192}\text{Hg}$ .

$E_\gamma$ (keV)	$\tau$ (ps)	$B(E2)$ (W.u.) <sup>a</sup>	$Q_t$ (e b)	$(Q_t)_{\text{SF}}$ (e b) <sup>b</sup>
458.4	0.234(75)	2700( $\pm 1280$ )	22.0( $\pm 4.8$ )	26( $\pm 3$ )
495.9	0.184(40)	2310( $\pm 640$ )	20.6( $\pm 7.3$ )	> 24
532.0	0.129(45)	2310( $\pm 1240$ )	20.6( $\pm 4.3$ )	17( $\pm 4$ )
567.5	0.083(24)	2590( $\pm 1880$ )	21.8( $\pm 4.4$ )	16( $\pm 3$ )
602.0	0.080(20)	2000( $\pm 970$ )	19.1( $\pm 3.8$ )	14( $\pm 3$ )
634.9	0.060(24) <sup>c</sup>	2040( $\pm 1360$ )	19.3( $\pm 3.8$ )	> 8
668.2	0.049(13)	1930( $\pm 700$ )	18.7( $\pm 3.1$ )	15( $\pm 3$ )
700.0	0.046(20)	1630( $\pm 450$ )	17.2( $\pm 2.3$ )	9( $\pm 3$ )
730.4				
761.8	< 0.04 <sup>d</sup>	> 1500	> 6	...
791.9				

<sup>a</sup>W.u. denotes Weisskopf units.

<sup>b</sup>These values were obtained under the assumption of sidefeeding properties similar to those of the main band (see text for details).

<sup>c</sup>Derived from fit to preceding and succeeding transitions (see text).

<sup>d</sup>Effective lifetime, not corrected for sidefeeding. Obtained from fits to  $F(\tau)$  values and to line shapes of lower-lying transitions (see text for details).

well reproduced. A few details of the analysis are noteworthy. The 700-keV transition is the highest one for which a line-shape analysis was possible. However, fractions of full Doppler shift  $F(\tau)$  for the  $\gamma$  rays from the three highest SD states (730.4, 761.8, and 791.9 keV) were in good agreement with simulations using  $Q_t > 16$  e b. Similar lifetime constraints have also been obtained on these three states from the simultaneous fit to the 700- and 668-keV line shapes. The presence of the  $4^+ - 2^+$  and  $8^+ - 6^+$  transitions close to the 635-keV line (Fig. 1) prevented accurate fitting of its line shape. Since its lifetime influences the line shapes of the following transitions, it was possible to obtain a value from a fit of preceding and succeeding transitions in the cascade, a procedure which did not allow a reliable sidefeeding lifetime determination.

The lifetimes were transformed into transition quadrupole moments  $Q_t(I) = (1.22 \langle I020 | I-20 \rangle \tau E_\gamma^5)^{-1/2}$  assuming spin values adopted in Ref. 4. The  $Q_t$  values are presented in Table I and displayed as a function of  $\hbar\omega$  in Fig. 3(b). Table I also contains the transition probabilities  $B(E2, I \rightarrow I-2)$  normalized to the single-particle estimates. As can be seen from Fig. 3(b) the quadrupole moment  $Q_t$ , and hence the deformation, remain essentially constant over the entire frequency range.

This result rules out centrifugal stretching as an explanation for the rise in  $\mathcal{J}^{(2)}$ : This is illustrated by the dashed line in Fig. 3(b) where the values of  $Q_t$  have been derived assuming that the change in  $\mathcal{J}^{(2)}$  is attributed entirely to a variation in deformation.<sup>14</sup> As already discussed by Ye *et al.*,<sup>4</sup> calculations without pairing, such as those by Chasman or Aberg,<sup>15</sup> give proton and neutron contributions to  $\mathcal{J}^{(2)}$  which remain essentially constant with  $\hbar\omega$ . Thus, the increase in  $\mathcal{J}^{(2)}$  cannot be ac-

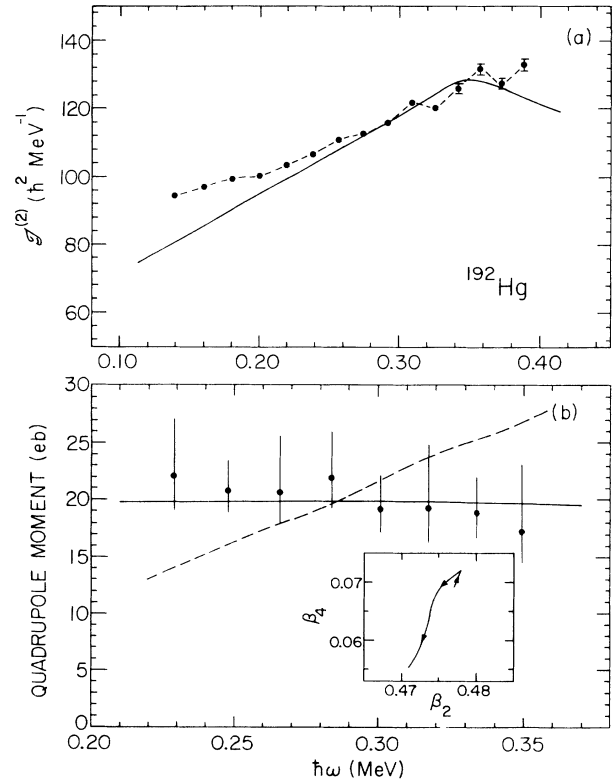


FIG. 3. (a) Comparison between the measured and calculated (solid line) dynamic moments of inertia  $\mathcal{J}^{(2)}$  as a function of rotational frequency  $\hbar\omega$  in the SD band of  $^{192}\text{Hg}$ . (b) Comparison between the measured and calculated transition quadrupole moments  $Q_t$  in the SD band of  $^{192}\text{Hg}$ . The dashed line represents a calculation assuming that the rise in  $\mathcal{J}^{(2)}$  is due to a change in deformation only (see text); the solid line is the result of the cranked shell-model calculation discussed in the text. Inset: The calculated change in the deformation parameters  $\beta_2$  and  $\beta_4$  over the frequency range of interest. The arrows point towards increasing frequencies.

counted for by the occupation of specific high- $j$  orbitals. This points to the need to examine the effects of pairing.

The results can be understood within the framework of cranked Woods-Saxon Strutinsky calculations with pairing. The approach has been presented in detail in Ref. 6 and has been applied with some success to the description of SD bands in  $^{191}\text{Hg}$  by Carpenter *et al.*<sup>2</sup> and in  $^{194}\text{Hg}$  by Riley *et al.*<sup>5</sup> Figure 3(a) compares the calculated dynamic moment of inertia with the data. The rise in the calculated  $\mathcal{J}^{(2)}$  can be ascribed to the combined alignment of a pair of  $N=6$  ( $i_{13/2}$ ) protons and of a pair of  $N=7$  ( $j_{15/2}$ ) neutrons within the frequency range under consideration. The evolution of the nuclear shape with  $\hbar\omega$  was also calculated. The inset in Fig. 3(b) illustrates that within the frequency range of interest the predicted changes in  $\beta_2$  and  $\beta_4$  are very small. Note that theoretical values of  $\beta_2$  have to be multiplied by 1.1 in order to compare with experiment.<sup>6</sup> The resulting  $Q_t$  values agree well with the measured values as is shown

by the solid line in Fig. 3(b). The success of the calculations in reproducing all aspects of the data allows us to propose that quasiparticle alignments and the resulting changes in pairing represent a major factor contributing to the rise in  $\mathcal{J}^{(2)}$  in  $^{192}\text{Hg}$  and, probably, in other nuclei in this region.

As already mentioned above, DSAM measurements also provide information on the sidefeeding lifetimes. In the present case, sidefeeding occurs mainly into the highest-spin states. Thus, the most accurate information can be derived from the fits to the line shapes of the highest transitions. If the sidefeeding is assumed to come from rotational bands with the same  $\mathcal{J}^{(2)}$  as the SD band (a similar assumption is often used for the description of the sidefeeding into rotational cascades; see, e.g., Refs. 11 and 13), then the resulting transition quadrupole moment for the sidefeeding can be derived from the sidefeeding parameter  $(Q_t^2/\mathcal{J}^5)_{\text{SF}}$ . The corresponding values  $(Q_t)_{\text{SF}}$  are also given in Table I. The average values for  $Q_t$  and  $(Q_t)_{\text{SF}}$  differ slightly, 20 vs 16 e b. This difference may reflect the proposed admixture<sup>16</sup> between SD levels and states of smaller deformation above the yrast line. The smaller  $(Q_t)_{\text{SF}}$  value could also be due, at least in part, to the approximation used in the description of the sidefeeding cascade in terms of a rotational band which feeds the SD band directly.

In conclusion, the present measurements demonstrate that the SD shape of  $^{192}\text{Hg}$  is not altered appreciably under rotation. The observed rise in the value of  $\mathcal{J}^{(2)}$  with  $\hbar\omega$  is consistent with results of the cranked Woods-Saxon Strutinsky model with pairing.

The authors wish to thank Hans Emling for the use of the code LILIFI and for many fruitful discussions. Discussions with Mark Riley and Dick Chasman are gratefully acknowledged. This work was supported in part by the Department of Energy, Nuclear Physics Division,

under Contracts No. W-31-109-ENG-38, No. DE-AC07-76IDO1570, and No. DE-FG02-87ER40346, by the National Science Foundation under Grant No. PHY88-02279, by the Polish Ministry of National Education under Contract No. CPBP 01.09, and by the Swedish Natural Science Research Council.

---

<sup>(a)</sup>Permanent address: Hampton University, Hampton, VA 23668.

<sup>1</sup>P. J. Nolan and P. J. Twin, *Annu. Rev. Nucl. Part. Sci.* **38**, 533 (1988).

<sup>2</sup>E. F. Moore *et al.*, *Phys. Rev. Lett.* **63**, 360 (1989); M. P. Carpenter *et al.*, *Phys. Lett. B* (to be published).

<sup>3</sup>M. W. Drigert *et al.* (to be published).

<sup>4</sup>D. Ye *et al.*, *Phys. Rev. C* **41**, 13 (1990); J. A. Becker *et al.*, *Phys. Rev. C* **41**, 9 (1990).

<sup>5</sup>M. Riley *et al.*, *Nucl. Phys. A* (to be published); C. Beausang *et al.*, *Z. Phys.* (to be published).

<sup>6</sup>W. Nazarewicz *et al.*, *Phys. Lett. B* **255**, 208 (1989); *Nucl. Phys. A* **503**, 285 (1989).

<sup>7</sup>T. Bengtsson *et al.*, *Phys. Lett. B* **208**, 39 (1988).

<sup>8</sup>R. M. Diamond *et al.*, *Phys. Rev. C* **41**, 1327 (1990).

<sup>9</sup>R. V. F. Janssens *et al.* (to be published).

<sup>10</sup>H. Emling *et al.*, in *Proceedings of the Twenty-Second School on Physics, Zakopane, Poland, 1987*, edited by R. Broda and Z. Stachura (Instytut Fizyki Jądrowej w Krakowie Report No. IFJ 1956/PL), p. 151.

<sup>11</sup>H. Emling *et al.*, *Phys. Lett. B* **217**, 33 (1989).

<sup>12</sup>J. F. Ziegler, J. P. Biersack, and U. Littmark, *The Stopping and Range of Ions in Solids* (Pergamon, New York, 1985).

<sup>13</sup>H. Emling *et al.*, *Nucl. Phys. A* **419**, 187 (1984).

<sup>14</sup>G. Leander (private communication).

<sup>15</sup>R. R. Chasman, *Phys. Lett. B* **219**, 227 (1989); S. Aberg, *Phys. Scr.* **25**, 23 (1982); (private communication).

<sup>16</sup>K. Schiffer *et al.*, *Z. Phys. A* **332**, 17 (1989).